

# Coupling Schemes for Heterogeneous Integration of III-V Membrane Devices and Silicon-on-Insulator Waveguides

G. Roelkens, *Student Member, IEEE*, Dries Van Thourhout, *Member, IEEE*, and Roel Baets, *Senior Member, IEEE*

**Abstract**—We present and numerically analyze two schemes for efficient, large-bandwidth, and fabrication-tolerant optical coupling of bonded III-V membrane active components to an underlying nanophotonic waveguide circuit in silicon-on-insulator (SOI). Coupling of active membrane components to passive waveguides enables the integration of ultracompact passive waveguide circuits and active optoelectronic devices.

**Index Terms**—Heterogeneous integration, nanophotonics, silicon-on-insulator (SOI), thin-film optoelectronic components.

## I. INTRODUCTION

THE INTEGRATION of different optical functions on a photonic IC fabricated using high-yield wafer-scale technologies is expected to result in systems-on-a-chip that outperform their discrete and die-level integrated counterparts in compactness, performance, complexity, and cost. As a general system contains both active functions (amplification, switching, modulation, light emission, and detection) and passive optical waveguides, different materials need to be integrated into a single system.

High-index-contrast waveguides are very attractive to be used in the passive waveguide layer. Optical circuits based on photonic wires and photonic crystals make ultracompact optical functions possible, and the high index contrast allows very-large-scale integration of optical waveguides. Recently, low waveguide-propagation losses were obtained for silicon-on-insulator (SOI) high-index-contrast nanophotonic waveguide structures [1], [2]. Moreover, these waveguide structures are defined by deep ultraviolet (UV) lithography, the workhorse of CMOS technology [3], and wafer-scale processes. Based on the considerations above, in this paper, we focus on the coupling of optoelectronic devices and passive nanophotonic waveguides in SOI.

The choice of active layer material is determined by the optical transparency of the SOI waveguide ( $\lambda > 1.1 \mu\text{m}$ ) at

the active-material bandgap wavelength. We will concentrate on InP/InGaAsP active devices with a bandgap wavelength around  $1.55 \mu\text{m}$ .

The application of this integration technique is not limited to complex optical systems-on-a-chip. In future CMOS technology nodes, the metal interconnections are no longer expected to satisfy the bandwidth needs, especially for the global interconnection level, where interconnection distances are the largest. According to the International Technology Roadmap for Semiconductors (ITRS) roadmap [4], a promising approach is the use of a photonic interconnection layer on top of CMOS. This layer may contain on-chip sources and detectors coupled to an optical waveguide layer.

## II. HETEROGENEOUS INTEGRATION

### A. Integration Technique

Integration of different materials into a single system can be accomplished in a variety of ways. Direct growth of InP material on an Si substrate results in high dislocation densities due to the large mismatch in lattice constant. This optically degrades the active layers. Eutectic bonding [5], using metal alloys, results in nontransparent bonding layers. In direct wafer bonding [6], two polished wafer surfaces are fused together. This technique allows an optically transparent bonding interface but requires advanced chemical-mechanical polishing (CMP) processing to bond processed SOI waveguide substrates and InP dies. An alternative approach, which is assumed in this paper, is to use an optically transparent adhesive layer, which is spin coated onto the substrates and used as a bonding agent by curing the adhesive.

### B. Membrane Device Definition

As the size of industrially available CMOS wafers and SOI waveguide wafers (up to 300 mm) differ from the size of InP wafers (50–75 mm), a “die-to-wafer” bonding approach is needed. This implies that InP dies need to be picked, placed, and bonded on an SOI wafer. As our intention is to couple active devices to nanophotonic waveguide structures, alignment is very stringent. This can only be achieved through lithographic alignment of SOI structures and active devices. Therefore, unprocessed InP dies are bonded to the SOI waveguide substrate, epi-layers down, and then, the InP substrate is removed using mechanical and chemical thinning until an

Manuscript received May 25, 2004; revised June 22, 2005. This work was supported in part by the European Union under the Information Society Technologies (IST) project Photonic Interconnect layer on CMOS (PICMOS) (FP6-2002-IST-1-002131). The work of G. Roelkens was supported by the Fund for Scientific Research (FWO) and the Interuniversity Attraction Poles (IAP)-Photon network. The work of D. Van Thourhout was supported by the Federal Science Policy Office under a return grant.

The authors are with the Department of Information Technology (INTEC), Ghent University–Interuniversity MicroElectronics Center (IMEC), B-9000 Ghent, Belgium (e-mail: gunther.roelkens@intec.ugent.be).

Digital Object Identifier 10.1109/JLT.2005.856231



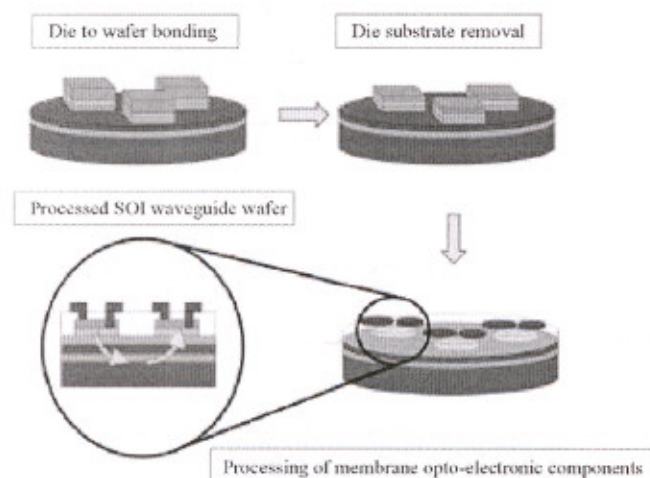


Fig. 1. Processing sequence for heterogeneous integration of III-V components and SOI waveguides.

etch-stop layer is reached. This leaves a thin active film that can be processed subsequently, with structures lithographically aligned to the SOI waveguides. As the bonded dies are unprocessed, positioning accuracy is less stringent. The processing sequence is shown in Fig. 1.

### III. COUPLING III-V AND SOI

As different types of active devices need to be integrated in a general system, the coupling method will differ for each type of device. An important distinction is the direction of the optical path in the active component. If the optical path is perpendicular to the waveguiding direction in the SOI (e.g., a heterogeneously integrated vertical cavity surface emitting laser (VCSEL)), a beam turning coupler is needed to couple light from III-V components to SOI and vice versa. In this paper however, we focus on in-plane optoelectronic devices.

A usable coupling scheme needs to be efficient and compact to have a large optical bandwidth and to be fabrication tolerant. The tolerance on the bonding-layer thickness is a very important issue. Polarization independence is not required in a photonic interconnection-layer application with on-chip sources, while a polarization diversity configuration can be applied to systems-on-a-chip for telecom applications [7]. In these configurations, the incoming unpolarized light is split into two beams with an orthogonal polarization state, and both are subsequently, independently processed in separate but identical devices and finally recombined.

Different ways of coupling light between the active components and the passive circuitry can be envisioned. The use of a grating structure to diffract guided waves to radiation modes and vice versa can result in very compact structures but has a reduced efficiency due to the limited directionality of the gratings and shows tight fabrication tolerances on both gratings due to the need for matching the grating angles and grating coupling lengths. The use of (grating-assisted) vertical directional couplers can be highly efficient but is considered equally fabrication intolerant due to the periodic power exchange between both waveguides. This results in a low bonding-layer

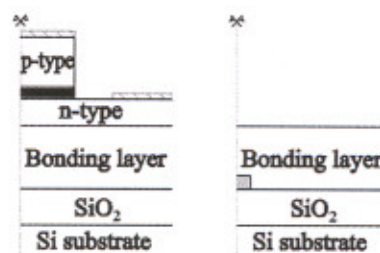


Fig. 2. (Left) InP membrane waveguide and (right) single-mode high-index-contrast SOI waveguide.

thickness tolerance and the stringent requirement of phase matching two high-index-contrast waveguides in different material systems.

In the following sections, two coupling schemes based on adiabatic tapers will be presented. The use of adiabatic tapers as mode transformers makes an efficient coupling with large optical bandwidth possible and allows a tradeoff between fabrication tolerance and design compactness.

The first design is based on a thin-film spin-on glass (SOG) adhesive bonding layer. Bonding-layer thicknesses below  $0.5 \mu\text{m}$  have been shown in [8]. The second design is based on a thick-film benzocyclobutene (BCB) bonding. Bonding-layer thickness above  $1 \mu\text{m}$  is readily achievable [9]. Both materials are used in the CMOS industry, respectively, as metal isolation layer and passivation material. The coupling schemes are equally applicable to other transparent bonding materials with comparable layer thickness and optical properties.

The assumed active thin-film layer structure consists of six  $6.4\text{-nm}$ -thick,  $1\%$  compressively strained  $\text{In}_{0.76}\text{Ga}_{0.24}\text{As}_{0.79}\text{P}_{0.21}$  quantum wells separated by  $5.5\text{-nm}$ -thick  $\text{In}_{0.71}\text{Ga}_{0.29}\text{As}_{0.55}\text{P}_{0.45}$  barrier layers. The separate confinement layers are assumed  $50\text{-nm}$ -thick  $\text{In}_{0.83}\text{Ga}_{0.17}\text{As}_{0.37}\text{P}_{0.63}$  layers. The first and last barrier layers are  $17\text{-nm}$  thick [10]. The active waveguide is assumed  $2.5\text{-}\mu\text{m}$  wide. The thickness of the cladding layers depends on the coupling mechanism used.

The coupling schemes presented transform the fundamental mode of the active ridge structure to the fundamental mode of an SOI waveguide with a  $220\text{-nm}$ -thick Si core layer. The bonded active ridge waveguide and a  $600\text{-nm}$ -wide single-mode SOI waveguide are shown in Fig. 2 on the same scale. Notice the large dimensional mismatch between both waveguides.

The simulations were performed using a fully vectorial eigenmode expansion tool [11]. TE polarization and, unless noted otherwise, a wavelength of  $1.55 \mu\text{m}$  was assumed.

#### A. SOG-Bonding Coupling Scheme

The proposed coupling scheme is presented in Fig. 3. It consists of a double adiabatic-taper structure to transform the fundamental waveguide modes. The first taper transforms the active waveguide mode to the fundamental mode of a passive InP membrane waveguide. This waveguide is formed in the n-type contacting layer, so propagation losses due to free carrier absorption are small. Subsequently, light is coupled from the InP membrane to the SOI waveguide using an SOI adiabatic-taper coupler. This coupler is based on a



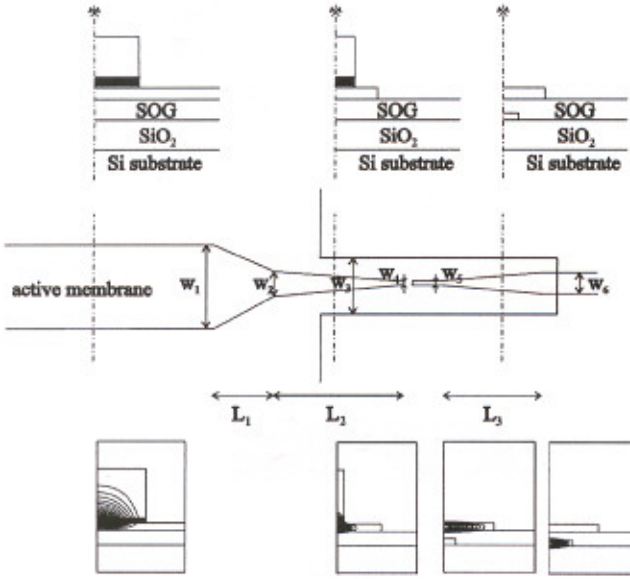


Fig. 3. SOG-bonding coupling scheme—layout and mode transformation.

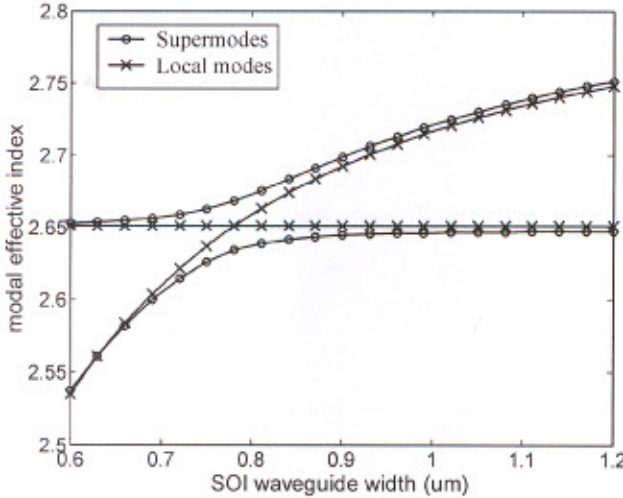


Fig. 4. SOI adiabatic-taper operation principle—modal effective indices.

phase-matching condition of the fundamental modes of the SOI waveguide and the InP membrane. As the thickness of the SOI waveguide is about  $\lambda/2n$  to be vertically single mode, the phase-matching condition implies that this is also needed for the InP membrane.

Fig. 4 shows the operation principle of the SOI adiabatic-taper structure. TE effective indices of the supermodes of taper structures, as well as the effective indices of the local modes, which are the modes of the uncoupled waveguides, are plotted versus SOI waveguide width. A 275-nm-thick InP membrane is assumed ( $w_4 = 2.5 \mu\text{m}$ ) separated from the SOI waveguide by a 300-nm-thick SOG layer ( $n = 1.4$ ). When one supermode is excited and that supermode is transformed adiabatically over the phase matching area, light is coupled from one waveguide to the other. The maximum adiabatic-taper angle is critically dependent on bonding-layer thickness, as shown in Fig. 5. While the exact taper length depends on taper waveguide shape, which is determined by the required tolerance of the

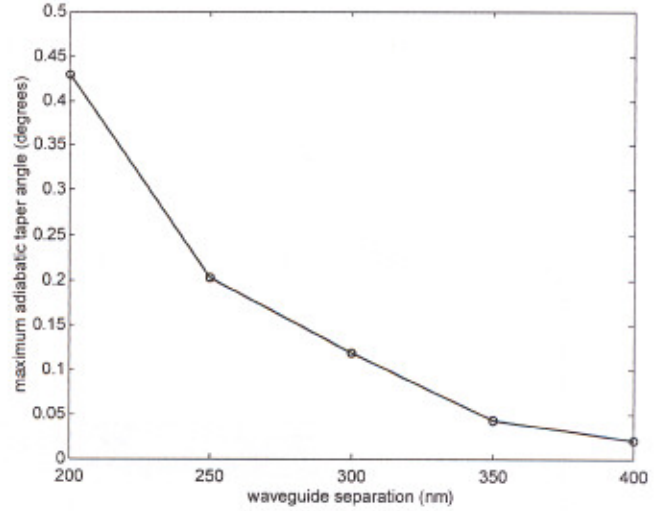


Fig. 5. Maximum adiabatic SOI taper angle versus waveguide separation for the SOG bonding coupling scheme.

TABLE I  
PARAMETERS WAVEGUIDE STRUCTURES: BCB BONDING  
VERSUS SOG BONDING

Parameter	Value	Parameter	Value
$w_{1,SOG}$	2.5 $\mu\text{m}$	$w_{1,BCB}$	2.5 $\mu\text{m}$
$w_{2,SOG}$	0.6 $\mu\text{m}$	$w_{2,BCB}$	1.8 $\mu\text{m}$
$w_{3,SOG}$	2.5 $\mu\text{m}$	$w_{3,BCB}$	3.5 $\mu\text{m}$
$w_{4,SOG}$	0.2 $\mu\text{m}$	$w_{4,BCB}$	1.1 $\mu\text{m}$
$w_{5,SOG}$	0.6 $\mu\text{m}$	$w_{5,BCB}$	0.05 $\mu\text{m}$
$w_{6,SOG}$	1.2 $\mu\text{m}$	$w_{6,BCB}$	0.3 $\mu\text{m}$
$L_{1,SOG}$	80 $\mu\text{m}$	$L_{1,BCB}$	80 $\mu\text{m}$
$L_{2,SOG}$	50 $\mu\text{m}$	$L_{2,BCB}$	180 $\mu\text{m}$
$L_{3,SOG}$	160 $\mu\text{m}$	$L_{3,BCB}$	130 $\mu\text{m}$

design to fabrication variations, a waveguide separation below 0.4  $\mu\text{m}$  is needed to design compact and efficient couplers. Parameters for adiabatic InP waveguide-mode transformation and for an adiabatic linear SOI taper are given in Table I for a waveguide separation of 300 nm. The narrow InP taper tips can be defined using deep UV lithography. Simulations show a less than 1-dB coupling loss over the 1500–1600-nm wavelength range. In these simulations, the wavelength dependence of the used materials was also taken into account. As this coupling scheme shows very low reflection, it can be used for the heterogeneous integration of semiconductor optical amplifiers and passive nanophotonics.

#### B. BCB Bonding Coupling Scheme

Because of the critical dependence on the bonding-layer thickness in the SOG bonding coupling scheme, an alternative coupling scheme that reduces this dependence is presented in Fig. 6. The structure is based on bonding using BCB ( $n = 1.55$ ). Due to the higher refractive index of the BCB compared to the  $\text{SiO}_2$  buffer layer ( $n = 1.45$ ), an additional



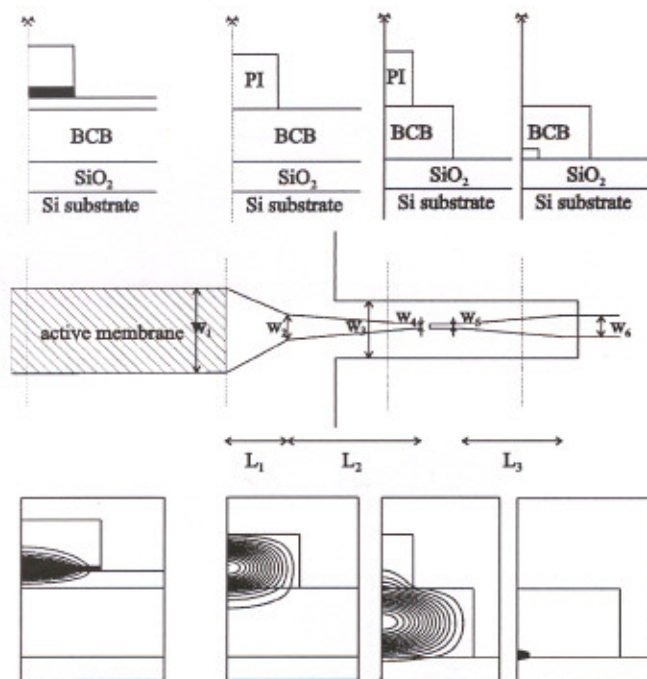


Fig. 6. BCB bonding coupling scheme—layout and mode transformation.

waveguide is formed. The coupling mechanism is conceptually equivalent to the SOG bonding coupling scheme and transforms the waveguide mode using a double adiabatic-taper structure. The first adiabatic taper is implemented in a higher refractive-index polymer waveguide layer (referred to as PI in Fig. 6, as a proper polyimide is a potential candidate for this waveguiding layer), which is butt-coupled to the active ridge waveguide [12]. This implies an intrinsic reflection at the semiconductor/polymer interface and a reduced efficiency due to butt-coupling loss. This loss is a function of the index contrast between the polymer core and the BCB cladding layer because of the mode profile mismatch between the fundamental waveguide modes in the active membrane and the polymer waveguide. Reflection and transmission at the semiconductor/polymer interface are shown in Fig. 7 as a function of the PI/BCB index contrast. The III-V waveguide cladding-layer thickness and polymer waveguide height are optimized for each index difference to obtain the lowest loss. This graph shows that for a sufficiently high index contrast, the coupling can be efficient. Fig. 8 shows the dependence of the maximum adiabatic-taper angle of the SOI waveguide as a function of bonding-layer thickness. Compared to Fig. 5, this dependence is drastically reduced. Using the parameters noted in Table I, the transmission loss of the double adiabatic-taper structure is simulated to be below 0.5 dB over the 1500–1600-nm wavelength range. A refractive-index difference between polymer core and cladding of 0.05 over the whole wavelength range is assumed. The bonding layer is assumed to be 3- $\mu\text{m}$  thick ( $w_4 = 3.5 \mu\text{m}$ ), while the optimized polymer core thickness is 2.3  $\mu\text{m}$ . The narrow SOI taper tip is needed for low insertion loss. Definition of these taper tips requires e-beam lithography [13]. The intrinsic reflection at the semiconductor–polymer interface enables the heterogeneous integration of edge-

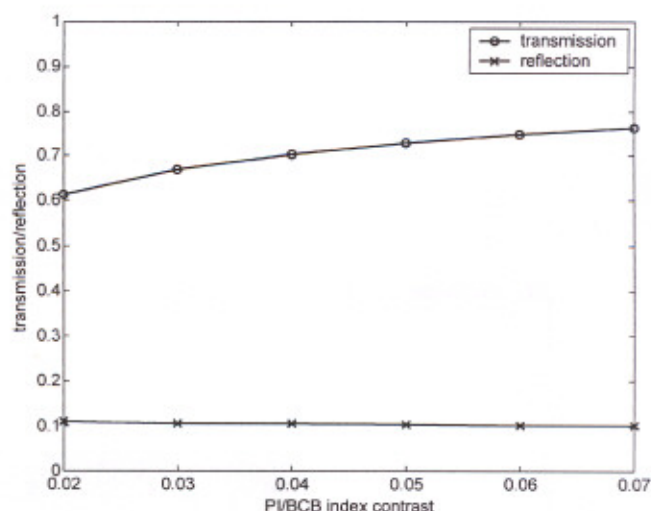


Fig. 7. Influence of the PI/BCB index contrast on the transmission and reflection at the polymer/III-V interface.

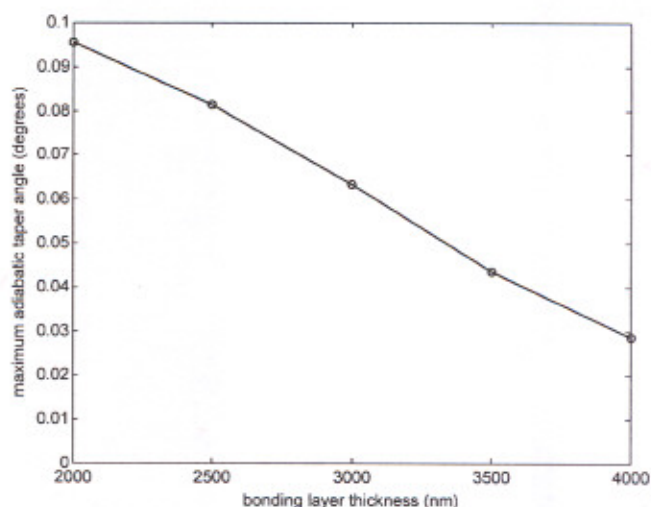


Fig. 8. Maximum adiabatic-taper angle versus bonding-layer thickness for the BCB bonding coupling scheme.

emitting lasers and passive nanophotonics. In applications where reflection into the active waveguide has to be avoided, angled facets can be used.

#### IV. CONCLUSION

Two schemes are presented to efficiently couple III-V active components and SOI photonic wires. As the proposed coupling schemes are based on adiabatic transitions, both conservative designs can be made, depending on the achievable process control concerning thickness, width, refractive index, and misalignment of waveguides. More compact devices can be fabricated if stringent process control is available. The first bonding scheme requires a thin bonding layer ( $< 0.4 \mu\text{m}$ ) and has no intrinsic reflections, which makes it useful for the heterogeneous integration of semiconductor optical amplifiers and passive nanophotonics. The second design is more tolerant to bonding-layer thickness variation and has an intrinsic



reflection, which makes it useful for the heterogeneous integration of edge-emitting lasers.

#### ACKNOWLEDGMENT

The authors would like to thank Prof. M. K. Smit for the fruitful discussions.

#### REFERENCES

- [1] P. Dumon, W. Bogaerts, V. Wiaux, J. Wouters, S. Beckx, J. Van Campenhout, D. Taillaert, B. Luyssaert, P. Bienstman, D. Van Thourhout, and R. Baets, "Low-loss SOI photonic wires and ring resonators fabricated with deep UV lithography," *IEEE Photon. Technol. Lett.*, vol. 16, no. 5, pp. 1328–1330, May 2004.
- [2] K. K. Lee, D. R. Lim, and L. C. Kimerling, "Fabrication of ultralow-loss Si/SiO<sub>2</sub> waveguides by roughness reduction," *Opt. Lett.*, vol. 26, no. 23, pp. 1888–1890, Dec. 2001.
- [3] W. Bogaerts, V. Wiaux, D. Taillaert, S. Beckx, B. Luyssaert, P. Bienstman, and R. Baets, "Fabrication of photonic crystals in silicon-on-insulator using 248-nm deep UV lithography," *IEEE J. Sel. Topics Quantum Electron.*, vol. 8, no. 4, pp. 928–934, Jul.–Aug. 2002.
- [4] [Online]. Available: <http://public.itrs.net>
- [5] H. C. Lin, W. H. Wang, K. C. Hsieh, and K. Y. Cheng, "Metallic wafer bonding for the fabrication of long-wavelength vertical-cavity surface-emitting lasers," *J. Appl. Phys.*, vol. 92, no. 7, pp. 4132–4134, May 2002.
- [6] C. Monat, C. Seassal, X. Letartre, P. Viktorovitch, P. Regreny, M. Gendry, P. Rojo-Romeo, G. Hollinger, E. Jalaguier, S. Pocas, and B. Aspar, "InP 2D photonic crystal microlasers on silicon wafer: Room temperature operation at 1.55  $\mu\text{m}$ ," *Electron. Lett.*, vol. 37, no. 12, pp. 764–765, Jun. 2001.
- [7] D. Taillaert, H. Chong, P. Borel, L. Frandsen, R. De La Rue, and R. Baets, "A compact two-dimensional grating coupler used as a polarization splitter," *IEEE Photon. Technol. Lett.*, vol. 15, no. 9, pp. 1249–1251, Sep. 2003.
- [8] H. C. Lin, K. L. Chang, G. W. Pickrell, K. C. Hsieh, and K. Y. Cheng, "Low temperature wafer bonding by spin on glass," *J. Vac. Sci. Technol. B*, vol. 20, no. 2, pp. 752–754, Mar/Apr. 2002.
- [9] F. Niklaus, P. Enoksson, E. Kälvesten, and G. Stemme, "Low-temperature full wafer adhesive bonding," *J. Micromech. Microeng.*, vol. 11, no. 2, pp. 100–107, Mar. 2001.
- [10] P. Abraham, "Study of temperature effects on loss mechanisms in 1.55  $\mu\text{m}$  laser diodes with InGaP electron stopper layer," *Semicond. Sci. Technol.*, vol. 14, no. 5, pp. 419–424, 1999.
- [11] FIMMPROP3D by PhotonDesign.
- [12] H.-F. Kuo, S.-Y. Cho, J. Hall, and N. M. Jokerst, "InP/InGaAsP MQW thin film edge emitting lasers for embedded waveguide chip to chip optical interconnections," in *Proc. Lasers and Electro-Optics Society (LEOS) Conf.*, Tucson, AZ, 2003, vol. 1, pp. 63–64.
- [13] T. Shoji, T. Tsuchizawa, T. Watanabe, K. Yamada, and H. Morita, "Spot-size converter for low-loss coupling between 0.3  $\mu\text{m}$  square Si wire waveguides and single mode fibers," in *Proc. 15th Annu. Meeting IEEE Lasers and Electro-Optics Society*, Glasgow, U.K., 2002, vol. 1, pp. 289–290.



**G. Roelkens** (S'02) received the electronic engineering degree from Ghent University, Ghent, Belgium, in 2002.

Since 2002, he has been with the Department of Information Technology (INTEC), Ghent University. He is currently working in the field of heterogeneous integration.



**Dries Van Thourhout** (M'01) received the physical engineering and the Ph.D. degrees from Ghent University, Ghent, Belgium, in 1995 and 2002, respectively.

During 2000 to 2002, he was with Lucent Technologies, Bell Laboratories, Crawford Hill, NJ, working on the design, processing, and characterization of InP–InGaAsP monolithically integrated devices. In October 2002, he joined the Department of Information Technology (INTEC), Ghent University, where his work concentrates on integrated optoelectronic devices.



**Roel Baets** (M'88–SM'96) received the degree in electrical engineering from Ghent University, Ghent, Belgium, in 1980, the M.Sc. degree in electrical engineering from Stanford University, Stanford, CA, in 1981, and the Ph.D. degree from Ghent University, in 1984.

Since 1981, he has been with the Department of Information Technology (INTEC), Ghent University. Since 1989, he has been a Professor with the engineering faculty, Ghent University. From 1990 to 1994, he was also a part-time Professor with the

Technical University of Delft, Delft, The Netherlands. He has mainly worked in the field of photonic components. With about 300 publications and conference papers as well as about ten patents, he has made contributions to the design and fabrication of III–V semiconductor laser diodes, passive guided wave devices, photonic integrated circuits, and micro-optic components. He leads the Photonics Group at Ghent University-INTEC (which is an associated lab of IMEC), working on the photonic devices for optical communication and optical interconnect.

Dr. Baets is a member of the Optical Society of America, the IEEE Lasers and Electro-Optics Society (LEOS), SPIE, and the Flemish Engineers Association. He has been a member of the program committees of OFC, ECOC, IEEE Semiconductor Laser Conference, ESSDERC, CLEO-Europe, IPR, and the European Conference on Integrated Optics. He was chairman of the IEEE-LEOS Benelux chapter from 1999 to 2001. Currently, he is a member of the Board of Governors of IEEE LEOS.